

BIBLIOTHÈQUE

TRI-PP-85-50  
Jun 1985

UNIVERSITY OF GENEVA



U - 2 -

Elastic scattering of polarised protons from  $^3\text{He}$  at intermediate energies\*

CM-P00067362

I. INTRODUCTION

The study of few-nucleon systems at intermediate energies can be particularly useful in providing information regarding the nuclear interaction. With only a few nucleons present, the theoretical analysis is relatively simple and can be dealt with in more detail. Yet most aspects of the nuclear interaction are still present in such systems and can be examined with the aim to gain insight into more complex systems and reactions. Considerable data are now available at intermediate energies on the few-nucleon systems of  $^2\text{H}$  and  $^4\text{He}$ , and to a lesser extent  $^3\text{H}$  and  $^3\text{He}$ . Ideally, one would like to use the data for the N-N interaction and formalism which already exist to explain the nucleon-nucleus interaction.

The multiple scattering theories of Glauber,<sup>1</sup> and Kerman, McManus, and Thaler<sup>2</sup> provide just such an approach. These theories make use of the free N-N scattering amplitudes and the wave function of the target nucleus. In the past, parameterised forms for the N-N scattering amplitudes and simple analytical forms for the wavefunctions have been used with encouraging success. However, these analyses have generally been limited to differential cross section data; the parameterisation for a spin dependent calculation not being readily apparent. In order to provide further data on the  $^3\text{He}$  system measurements were made of the differential cross section and analysing powers for elastic scattering of protons from  $^3\text{He}$  at incident proton energies of 200, 300, 415, and 515 MeV. The angular distributions measured cover the range  $15^\circ$  to  $150^\circ$  in the centre of mass. These data, together with data available from the literature in the energy range 100-1000 MeV,<sup>3-10</sup> were then analysed within the framework of the Glauber multiple scattering theory. Firstly, a simple spin independent calculation was performed using a parameterised form for

D.K. Hasell,† A. Bracco,† H.P. Gubler,§ W.P. Lee,¶ W.T.H. van Oers  
Department of Physics, University of Manitoba,  
Winnipeg, Manitoba, Canada R3T 2N2

R. Abegg, D.A. Hutcheon, C.A. Miller  
TRIUMF, Vancouver, British Columbia, Canada V6T 2A3

J.M. Cameron, L.G. Greeniaus, G.A. Moss  
Nuclear Research Centre, University of Alberta,  
Edmonton, Alberta, Canada T6G 2J1

M.B. Epstein, D.J. Margaziotis  
Department of Physics and Astronomy, California State University  
Los Angeles, California, 90032

Abstract

Differential cross sections and analysing powers for proton elastic scattering from  $^3\text{He}$  have been measured for proton scattering angles between  $15^\circ$  and  $150^\circ$  in the center of mass at incident proton energies of 200, 300, 415, and 515 MeV. The data have been analysed, together with data in the energy range 100-1000 MeV available from the literature, within the framework of the Glauber multiple scattering theory. Firstly, a simple spin independent calculation was performed using a parameterised form for the N-N scattering amplitudes. This provided reasonable agreement with the differential cross section data. Secondly, a more detailed calculation was performed incorporating spin dependence and using a complete set of N-N scattering amplitudes as determined from phase shift analyses. The agreement with the experimental data was not improved by the more detailed calculation. Possible reasons for this discrepancy are discussed.

the N-N interaction. This resulted in good agreement with the differential cross section data in general. Secondly, a more rigorous calculation was performed to include spin dependence using the scattering amplitudes derived from N-N phase shift analyses. Qualitative agreement was achieved between the calculated differential cross sections and analyzing powers and the data. However, the supposedly improved calculations generally underestimate the differential cross sections by 20-30% and are out of phase with the oscillations of the analyzing power data. Using N-N scattering amplitudes from different phase shift analyses had negligible effect on this discrepancy. Similarly, different forms for the  $^3\text{He}$  wave function could not account for the disagreement. Some qualitative improvements could be made by the choice of off-shell corrections. In the next section a brief description of the experimental setup, data reduction, and error analysis will be presented. Section III will describe the results obtained and compare them with existing data available from the literature. The theoretical model and the analysis will then be discussed in section IV followed by some conclusions.

## II. THE EXPERIMENT

The experiment was performed using polarized proton beams accelerated by the TRIUMF cyclotron to energies of 200, 300, 415, and 515 MeV. The beam position and direction were measured using wire profile monitors and by viewing a fluorescent screen which could be placed at the target position. The diameter of the beam at the target was about 5 mm. The incident proton beam polarization and integrated intensity were determined from the left and right counts derived from a polarimeter located upstream of the  $^3\text{He}$  target. A description of the  $^3\text{He}$  target system is given in Ref. 11. The polarimeter contained a 5 mg/cm<sup>2</sup> thick CH<sub>2</sub> target

and was previously calibrated against a Faraday cup. Typical proton beam polarizations were 65-75% depending on the energy at currents ranging from 1 to 15 namp. During the experiment the polarization of the incident proton beam was automatically changed from 'up' to 'off' to 'down' to 'off' cyclically. The  $^3\text{He}$  target thickness followed from measurements of the temperature of the target cell using germanium resistors embedded in the body of the cell and from the cell's physical dimensions measured with the same pressure differential. The target thicknesses so determined for the two target cells used in these measurements were 120±5 and 104±4 mg/cm<sup>2</sup>. The target cell radii both were 22 mm. The target cell could be raised or lowered remotely, thus permitting the  $^3\text{He}$  target cell to be replaced with an identical dummy cell in order to allow appropriate background subtractions. In addition the target cell could also be rotated around a central vertical axis in order to ensure that the scattered particles would not strike the side frames. The quadrupole-dipole magnetic spectrometer MRS was used to detect either the scattered protons or the recoil  $^3\text{He}$  particles. The spectrometer detection system consisted of a 0.8 mm thick plastic scintillator plus a 0.128 m by 0.128 m multiwire proportional chamber (MWPC) (with 2 mm wire spacing). The MWPC located before the quadrupole magnet-dipole magnet combination was used to define the solid angle. Typical solid angles were ~1 msr. The dipole magnet was followed by a set of 0.256 m by 1.024 m MWPC's (with 2 mm wire spacing) mounted about the focal plane of the magnetic spectrometer and a 25 mm thick plastic scintillator. The flight path through the spectrometer is ~11.0 m. Using the MWPC information the track of the detected particle was reconstructed and thus its position in the focal plane of the spectrometer was determined. The

momentum acceptance of the spectrometer was +12% to -10% of the central momentum. The energy resolution was ~0.25% which included effects due to the energy spread of the incident beam, kinematics, and multiple scattering in the target and the various covering foils. Protons were detected from forward angles to angles large enough that the corresponding recoil  $^3\text{He}$  particles had sufficient energy to be detected (~140 MeV). By detecting the recoil  $^3\text{He}$  particles a factor of ~3 was gained in the count rate due to the kinematic increase in the effective solid angle. In addition it was possible to perform the measurements at equivalent proton angles larger than the operating range of the magnetic spectrometer. The electronics for the experiment were interfaced via CAMAC to a data acquisition computer. Events satisfying specified limits for the time-of-flight and energy loss were logged on magnetic tape for subsequent analysis. During the experiment an on-line data analysis was performed to check on the performance of the electronics and data acquisition system. The yields of elastically scattered particles were calculated in the off-line reduction of the data by imposing more stringent tests and defining cuts. Events for which any of the MWPC planes had a missing wire-coordinate or events corresponding to firing of non-adjacent wires (with a gap greater than one wire) were rejected together with those outside the solid angle defining cut. The latter was chosen to correspond to the region of flat acceptance of the magnetic spectrometer. The yields were corrected for electronics and computer deadtime, detector inefficiencies, and reaction losses. Typical relative uncertainties of the differential cross section measurements are ~4-5% and these include uncertainties in the MWPC's efficiency (~1%), in the computer dead time correction (~1%), in the correction for reaction losses (0.4% in the case

of protons and 3% for  $^3\text{He}$ ), and uncertainties in the number of polarimeter counts used for normalization purposes (~1%), in the density of the  $^1\text{H}^3\text{He}$  (~3%), and finally the statistical error in the number of elastic scattering events observed. The absolute uncertainty in the normalization is ~6% and arises from uncertainties in the number of incident particles (~5%), in the target thickness (~1%), and in the solid angle (~1%). In addition the uncertainties in the detector angle is  $0.1^\circ$  and in the target rotation ~2.5°. The yields were calculated for each spin orientation and used to determine differential cross sections and analysing powers.

### III. RESULTS

The angular distributions of the differential cross sections and analysing powers for proton elastic scattering from  $^3\text{He}$  at 200, 300, 415, and 515 MeV are shown in Figs. 1 and 2 (numerical values can be obtained in tabulated form from the authors). The differential cross sections of the present work vary smoothly with angle. The first minimum can be clearly seen and there is evidence for the onset of the second minimum also. These minima can be explained by the Glauber theory to be due to interference between the single, double, and triple scattering terms. The analysing power angular distributions also vary quite smoothly and exhibit structure characteristic of interference of various scattering terms. Figure 3 shows the differential cross section data, as a function of the square of the four momentum transfer, for the present work along with data available from the literature in the energy range 100-1000 MeV. The variation with incident proton energy seems quite regular but at 415 MeV the data from the present experiment are 20-30% lower than the results of previous measurements (which were restricted to  $-t < 0.8 \text{ (GeV/c)}^2$ ). This discrepancy is larger than the sum of the

uncertainties in the absolute normalization of the two measurements.

However, the data from the present work match up quite well with the far backward angle data of Ref. 5. Near 600 MeV there are two sets of data available from the literature. The 582 MeV data of Ref. 6 are generally lower than the data of Ref. 8 at 600 MeV. At 1000 MeV there are also two independent measurements of the differential cross sections which are in fairly good agreement (Ref. 9 and 10).

#### IV. THEORETICAL ANALYSIS

The data obtained in the present work, together with the data available from the literature in the energy range (100-1000 MeV) were analysed within the framework of the Glauber multiple scattering theory. This theory assumed incident energies  $T$  sufficiently high so that  $T \gg V$ , where  $V$  is a measure of the strength of the interaction, and  $ka \gg 1$ , where  $k$  is the wave number and  $a$  is the effective width of the potential. Then, for small angle scattering such that  $\vec{k}-\vec{k}'$  is effectively perpendicular to  $\vec{k}$ , the scattering amplitude may be expressed as:

$$f(\vec{k}', \vec{k}) = \frac{-ik}{2\pi} \int e^{i(\vec{k}-\vec{k}') \cdot \vec{b}} (e^{i\chi(\vec{b})} - 1) d^2b, \quad (1)$$

where  $\vec{k}$  and  $\vec{k}'$  are the incident and outgoing wave vectors,  $\vec{b}$  is the impact parameter vector perpendicular to  $\vec{k}$ , and  $\chi$  is the total phase shift for the interaction. The total phase shift  $\chi$  is taken to be the sum of the phase shifts due to the incident nucleon scattering from each nucleon of the target individually. Thus for  ${}^3\text{He}$ :

$$\chi(\vec{b}, s_1, s_2, s_3) = \chi_1(\vec{b}-s_1) + \chi_2(\vec{b}-s_2) + \chi_3(\vec{b}-s_3) \quad (2)$$

where  $\vec{s}_1$ ,  $\vec{s}_2$ , and  $\vec{s}_3$  are the projections of the target nucleons' coordinates on the impact parameter plane. Expressing

$$T = 1 - e^{i\chi} \quad (3)$$

(often referred to as the profile function) then for  ${}^3\text{He}$  the total profile function can be written as:

$$T = T_1 + T_2 + T_3 - T_1T_2 - T_1T_3 - T_2T_3 + T_1T_2T_3 \quad (4)$$

The terms for single, double and triple scattering are clearly distinguished. The expression for the individual  $T$ 's can be obtained by applying Eq. (1) to the case of free N-N scattering.

$$T = \frac{1}{2\pi i q} \int e^{-i\vec{q} \cdot (\vec{b}-\vec{s})} f(\vec{q}) d^2q, \quad (5)$$

where  $\vec{q}$  is the momentum transfer, and  $f(\vec{q})$  is the free N-N scattering amplitude. Substituting the above expression for the individual profile functions, and Eq. (4) into Eq. (1) results in the scattering amplitude for  ${}^3\text{He}$  in terms of the free N-N scattering amplitudes. The various observables can be calculated from the expectation values of the scattering amplitude operating on the spin-isospin state of the target nucleus. The N-N scattering amplitudes operate on the spin and isospin terms while the integration over the nucleon coordinates produces a form factor for each term of the scattering amplitude. The calculation of the various observables then requires only the N-N scattering amplitudes and a wave function for  ${}^3\text{He}$ . This approach has been employed previously in the analysis of intermediate and high energy proton scattering from a variety of targets using a parameterised form of the N-N scattering amplitude given by:

$$f_{p,j} = \frac{\sigma_{p,j}^T}{4\pi} k(1+i\alpha_{p,j}) e^{i\beta_{p,j}t}; \quad j=p,n \quad (6)$$

where  $\sigma^T$  is the total cross section,  $k$  is the incident momentum,  $\alpha$  is the ratio of the real to the imaginary part of the scattering amplitude at

$0^\circ$ ,  $\beta$  is the slope parameter, and  $-t$  is the square of the four momentum transfer. In the first phase of the present analysis this parameterisation was used with values of  $\sigma^T, \alpha$ , and  $\beta$  as given in Table 1. They were obtained from the interactive phase shift analysis program SAID.12 The ground state wave function for  $^3\text{He}$  was taken as:

$$\psi = N e^{-c^2(r_1^2+r_2^2+r_3^2)}, \quad (7)$$

where  $N$  is the normalization constant,  $1/c=R=1.50$  fm is the rms radius for  $^3\text{He}$ , and the  $r_i$ 's are the nucleon coordinates within the  $^3\text{He}$  nucleus. The results of this rather simple calculation are shown in Fig. 3. The theoretical predictions overestimate the differential cross sections at lower energies and at 1000 MeV but generally agree quite well with the data. The positions of the minima are reproduced but not their depths. It should be noted that this parameterised form for the N-N scattering amplitudes does not contain any spin dependence, thus spin flip processes which might serve to fill in the minima are not considered. Similarly, charge exchange is not included in the calculation. Off-shell corrections were not incorporated at this stage. The same simple approach was previously used for comparison with the experimental data at 580 and 600 MeV (Ref. 6,7 and 8) with satisfactory results as well. In order to perform a more complete and rigorous theoretical analysis, Glauber calculations were made using the general form for the N-N scattering amplitudes which each consist of five independent terms resulting, in principle, in six independent terms of the  $p\text{-}^3\text{He}$  scattering amplitude. Since the necessary integrations over the transferred momenta in the double and triple scattering terms followed by the integration

over the coordinates of the target wave function can no longer be made analytically, the following approximation was used. The  $q$  dependence of the scattering amplitude  $f(q)$  was removed from the integral for the double and triple scattering terms by assuming that it could be replaced by an effective scattering amplitude taken at a momentum transfer  $q/2$  and  $q/3$ , respectively. The remaining integral over the target nucleon coordinates could again be performed analytically to produce the form factors for the single, double, and triple scattering terms. The expectation values for the single, double, and triple scattering terms multiplied by the appropriate form factor for all possible spin and isospin combinations were then evaluated. The results of these calculations, with values of the N-N scattering amplitudes obtained from Ref. 12, are shown in Figs. 4 and 5. The polarization data of Fig. 5 at 156 MeV are from Ref. 13. The agreement with the lower energy differential cross section data is quite good. This is a significant improvement over the simple Glauber calculations which overestimate the experimental differential cross sections. However, as the incident energy increases, the theoretical predictions considerably underestimate the experimental data. The only exceptions are the 1000 MeV comparisons. The positions of the minima given by the theoretical predictions are at smaller angles than experimentally measured. The calculated analysing power angular distributions have their forward maxima in good agreement with the experimental data but the calculated values go out of phase with the oscillations in the experimental data at larger angles. On average the results of the theoretically more complete calculations for the differential cross sections are significantly poorer than those of the simple Glauber

calculations. The disagreement at forward angles is particularly troublesome as the approximations should hold best in this region.

In order to study these discrepancies the contributions of the various terms which make up the calculations were examined individually. For this investigation an energy of 415 MeV was chosen, being the worst case in terms of agreement with experiment. Also the experimental differential cross section and analysing power data at this energy cover a broad angular range. Figure 6 illustrates the individual contributions of the single, double, and triple scattering terms. The single scattering contribution agrees well with the forward angle differential cross section data. It appears though that the double scattering contribution, while being significantly smaller, causes considerable interference effects in this region. The triple scattering term similarly interferes in the region of the second maximum and dominates at far backward angles.

The effect of using two different forms of the  $^3\text{He}$  wave function was next examined. A comparison was made with the predictions using the  $^3\text{He}$  wave function of Ref. 14 which is given by a sum of four Gaussians. Although this wave function better reproduces the  $^3\text{He}$  charge form factor than the simple Gaussian wave function, the latter gives Glauber predictions in slightly better agreement with the data. Off-shell corrections in a form given by Chew<sup>15</sup> and as used in Ref. 14 were also calculated: the shoulder in the curve at  $\sim 100^\circ$  as well as the back angle data are better reproduced with these corrections, but the region around  $60^\circ$  is better reproduced by the calculation without the off-shell corrections. However, the analysing power data show that the off-shell corrections enhance the depths of the minima. Spin-flip and charge exchange

processes appear to explain the filling in of the minima. This was clearly demonstrated by the 415 MeV calculations when these processes were removed from the full calculations.

Glauber calculations using N-N scattering amplitudes derived from phase shift analyses were performed by Bizard and Osmond<sup>16</sup> for the 415 and 600 MeV data and by Frascaria et al.<sup>10</sup> for the 600 and 1000 MeV data. Note that the present data cover a much larger range of the squared momentum transfer variable  $-t$ . The predictions at 415 and 600 MeV are lower than the experimental data while the 1000 MeV predictions agree with the data. The same features are observed in the present analysis, although more recent N-N scattering amplitudes were used. This appears to be consistent with the observation that the N-N scattering amplitudes derived from free N-N scattering are too small to reproduce nucleon-nucleus scattering observables; an observation earlier made in comparisons of Glauber and optical model analyses of 800 MeV proton elastic scattering from different nuclei.<sup>17</sup> The use of a more realistic  $^3\text{He}$  wave function could be considered. Yet a previous analysis made by Narbonne<sup>18</sup> with different  $^3\text{He}$  wave functions including S' and D state terms did not explain the disparity between theory and experiment. Similarly, improved off-shell corrections could be used. The introduction of intermediate nucleon resonances in the calculations should only be of importance at the higher energies.<sup>19</sup> Recently it has been shown<sup>20</sup> that a relativistic treatment of nucleon-nucleus scattering starting with the Dirac equation gives much better agreement with experiment. However, a formulation for the scattering of nucleons from a spin 1/2 target nucleus does not exist yet. The Glauber formulation as used here has assumed form factors independent of the spin and isospin of the scattering nucleons.

Certainly the neutron distribution within  ${}^3\text{He}$  will be different from that of the protons and also the spin distributions should be considered to be different. Such a formulation would require form factors dependent upon the spin and isospin rather than the simple matter distributions which have been used in the present work. A breakdown of the form factor in the various spin and isospin components has been used by Landau and Paž<sup>21</sup> in a microscopic, momentum space optical potential calculation for  $p$ - ${}^3\text{He}$  scattering which incorporates full spin-dependence of the N-N and  $p$ - ${}^3\text{He}$  interactions and which uses antisymmetrised N-N amplitudes. The  $t$ -matrices have on-shell behavior given by the N-N phase shifts and off-shell behavior from a realistic separable potential model. Qualitative agreement was found with the experimental data in the whole energy range 100 to 1000 MeV. Indications are that it would be possible to obtain better agreement with the data by varying the various form factors. However, verification of the validity of the form factors by an independent method would be required.

#### IV. CONCLUSION

The success of the simple Glauber model calculations over the more complete calculations for the differential cross sections implies that the parameterised N-N scattering amplitudes act as effective scattering amplitudes in the simple approach. Certainly the constant ratio of the real to the imaginary parts of the scattering amplitudes used in those calculations limits the degree of interference between the first and second order scattering which appears to be the problem with the more complete calculations. Improvements to the more complete calculations by explicitly carrying out the integration over the momentum transfer variable  $q$  rather than assuming an average value may give better agreement

with experiment. Consideration should also be given to formulate a relativistic description of nucleon scattering from a non-zero-spin target nucleus such as has been done with considerable success for nucleon scattering from a spin-zero target nucleus. Effects related to different  ${}^3\text{He}$  wave function forms, and excitation of nucleon resonances, would likely be too small to account for the discrepancies observed in comparing the present calculations with the experimental data.

REFERENCES

- \*Work supported in part by the Natural Sciences and Engineering Research Council of Canada, the National Science Foundation of the United States and the University of Manitoba Research Grants Committee.
- <sup>†</sup>Present address: Rutherford Appleton Laboratory, Chilton, Didcot, Oxfordshire, OX11 0XQ, United Kingdom.
- <sup>‡</sup>Present address: Dipartimento di Fisica, Università di Milano, Milano, 20133 Italy.
- <sup>§</sup>Present address: Sandoz AG, Pharma Dept, CH 4004, Basel, Switzerland.
- <sup>¶</sup>Present address: Department of Physics, University of California, Irvine, California, 92717
- <sup>1</sup>R.J. Glauber, in Lectures in Theoretical Physics, ed. by W.E. Brittin and L.G. Dunham, Interscience, New York, 1, 315 (1959).
- <sup>2</sup>A.K. Kerman, H. McManus, and R.M. Thaler, Ann. Phys., 8, 551 (1959).
- <sup>3</sup>N.P. Goldstein, A. Held, and D.G. Stairs, Can. J. Phys., 48, 2629 (1970).
- <sup>4</sup>H. Langevin-Joliot, Ph. Narboni, J.P. Didelez, G. Duhamel, L. Marcus, and M. Roy-Stephan, Nucl. Phys., A158, 309 (1970).
- <sup>5</sup>R. Frascaria, I. Brissaud, N. Marty, M. Morlet, F. Reide, A. Willis, R. Beurtey, A. Boudard, M. Garçon, G.A. Moss, Y. Terrien, and W.T.H. van Oers, Phys. Lett., 66B, 329 (1977).
- <sup>6</sup>M. Blecher, K. Gotow, E.T. Boschitz, W.K. Roberts, J.S. Vincent, P.C. Gugelot, and C.F. Perdrisat, Phys. Rev. Lett., 24, 1126 (1970).
- <sup>7</sup>E.T. Boschitz, W.K. Roberts, J.S. Vincent, M. Blecher, K. Gotow, P.C. Gugelot, C.F. Perdrisat, L.W. Swenson, and J.R. Priest, Phys. Rev., G6, 457 (1972).
- <sup>8</sup>J. Fain, J. Gardes, A. Lefort, L. Meritet, J.F. Pauty, G. Peynet, M. Querrou, F. Vazelle, and B. Ille, Nucl. Phys., A262, 413 (1976).
- <sup>9</sup>G.D. Alkhasov, S.I. Belostotsky, E.A. Damaskinsky, Yu.V. Dotsenko, O.A. Domchenkov, N.P. Kurpatekin, D. Legrand, V.N. Nikulin, O.E. Prokof'ev, M.A. Shuvaev, and S.S. Volkov, Phys. Lett., 85B, 43 (1979).
- <sup>10</sup>R. Frascaria, N. Marty, V. Comparat, M. Morlet, A. Willis, D. Legrand, D. Garreta, R. Beurtey, G. Bruge, P. Couvert, H. Gatz, A. Chaumeaux, J.C. Faivre, Y. Terrien, and R. Bertini, contribution IV. A. 12 to the Sixth International Conference on High Energy Physics and Nuclear Structure, Santa Fé and Los Alamos, 1975;
- R. Frascaria, L. Bimbot, Y. Le Bornec, M. Morlet, B. Tatischeff, N. Willis, D. Legrand, R. Beurtey, G. Bruge, P. Couvert, D. Garreta, G.A. Moss, and Y. Terrien, Contribution J30 to the Seventh International Conference on High Energy Physics and Nuclear Structure, Zürich, 1977;
- R. Frascaria, D. Legrand, V. Comparat, M. Morlet, N. Marty, and A. Willis, Nucl. Phys., A264, 445 (1976);
- G. Bruge, CEN-Saclay, Report DPh-N/ME/78-1, unpublished.
- <sup>11</sup>D.K. Hasell, R. Abege, B.T. Murdoch, W.T.H. van Oers, H. Postma, and J. Soukup, Nucl. Instr. Meth., 189, 341 (1981).
- <sup>12</sup>Obtained from the phase shift analyses of R.A. Arndt, L.D. Roper, R.A. Bryan, R.B. Clark, B.J. Verwest and P. Sigwell through a computer interactive dial-in system (SAID).
- <sup>13</sup>R. Frascaria, Ph. Narboni, V. Comparat, N. Marty, M. Morlet and A. Willis, Nuovo Cim. Lett., 2, 240 (1971).



<sup>14</sup>Ph. Narboni, Thesis, Centre d'Orsay, Université Paris-Sud, 1972, unpublished.

<sup>15</sup>G.F. Chew, Phys. Rev., 74, 809 (1948);

G.F. Chew and G.C. Wick, Phys. Rev., 85, 635 (1952).

<sup>16</sup>G. Bizard and A. Osmond, Nucl. Phys., A364, 333 (1981).

<sup>17</sup>G. Fäldt and A. Ingemarsson, Phys. Scripta, 25, 480 (1982).

<sup>18</sup>Ph. Narboni, Nucl. Phys., A205, 481 (1973).

<sup>19</sup>S.J. Wallace and Y. Alexander, Phys. Rev. Lett., 38, 1269 (1977).

<sup>20</sup>J.A. McNeil, J.R. Sheppard, and S.J. Wallace, Phys. Rev. Lett., 50, 1439 (1983);

J.R. Sheppard, J.A. McNeil, and S.J. Wallace, Phys. Rev. Lett., 50, 1443 (1983).

<sup>21</sup>R.H. Landau and M.J. Paez, Phys. Lett., B142, 235 (1984);

M.J. Paez and R.H. Landau, Phys. Rev., C29, 2264 (1984).

Table I.

Scattering parameters as used in the simple Glauber calculation.

$1/c = R = 1.50 \text{ fm}$							
$T_p$ (MeV)	$\sigma_{pp}^T$ (fm) <sup>2</sup>	$\alpha_{pp}$	$\beta_{pp}$ (GeV/c) <sup>-2</sup>	$\sigma_{pn}^T$ (fm) <sup>2</sup>	$\alpha_{pn}$	$\beta_{pn}$ (GeV/c) <sup>-2</sup>	
100.0	2.86	0.504	1.897	7.64	8.442	1.036	
156.0	2.30	0.175	1.630	4.89	6.935	0.907	
200.0	2.19	-0.068	1.323	4.10	5.199	0.686	
300.0	2.23	-0.093	0.843	3.48	2.530	0.295	
415.0	2.67	0.249	0.577	3.40	1.548	0.047	
515.0	3.40	0.753	0.413	3.57	1.560	-0.756	
582.0	3.88	1.191	0.302	3.71	1.679	-0.142	
600.0	4.00	1.110	0.275	3.75	1.712	-0.158	
715.0	4.55	1.949	0.117	3.92	1.945	-0.256	
1000.0	4.75	1.990	-0.144	4.02	2.133	-0.518	

FIGURE CAPTIONS

1. Differential cross section angular distributions for proton elastic scattering from  $^3\text{He}$  as measured in the present work. Relative errors are smaller than the size of the symbols.
2. Analysing power angular distributions for proton elastic scattering from  $^3\text{He}$  as measured in the present work. Relative errors are smaller than the size of the symbols unless shown.
3. Simple Glauber model calculations for the differential cross sections obtained in this work and available from the literature at intermediate energies.
4. Complete spin dependent Glauber calculations for the differential cross sections obtained in this work and available from the literature at intermediate energies.
5. Complete spin dependent Glauber calculations for the analysing powers obtained in this work and available from the literature at intermediate energies.
6. Single, double, and triple scattering contributions to the differential cross section at 415 MeV.

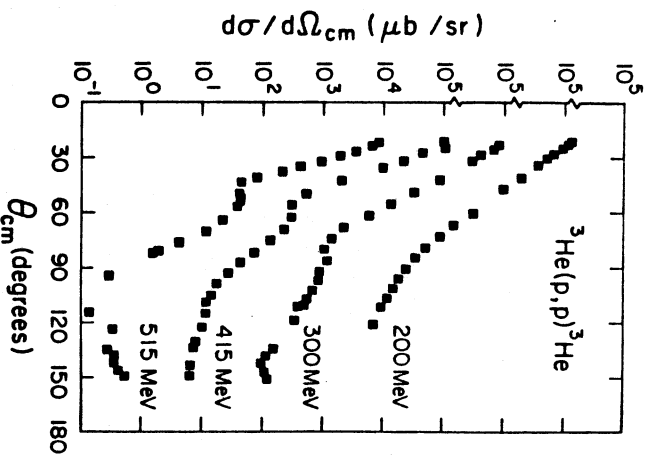


Fig. 1

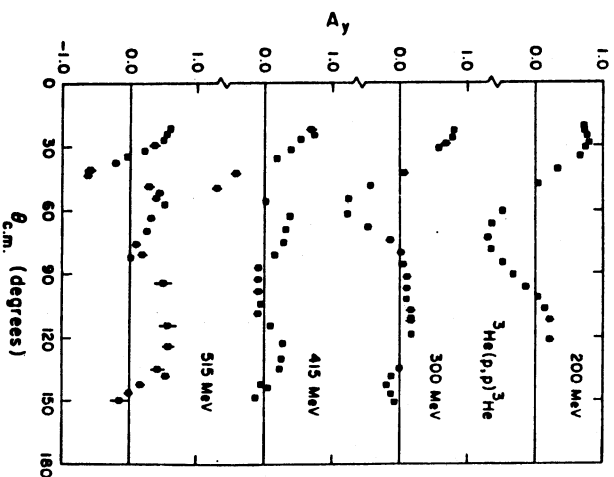


Fig. 2

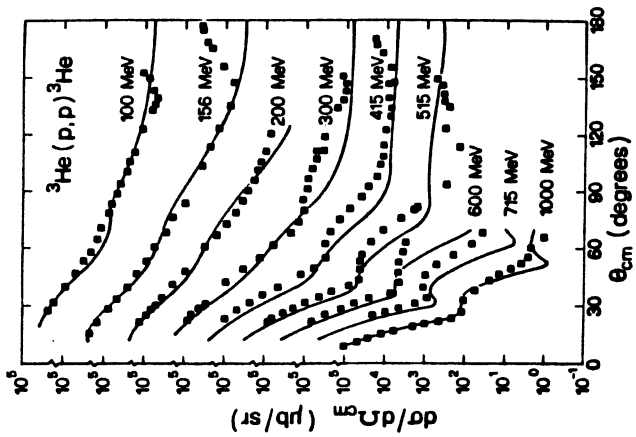


Fig. 4

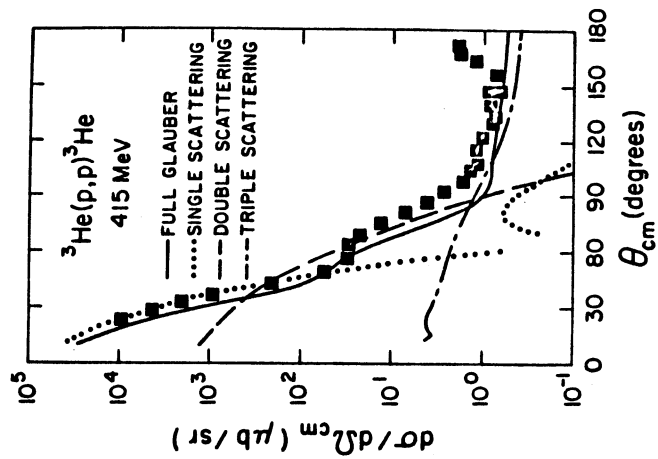


Fig. 6

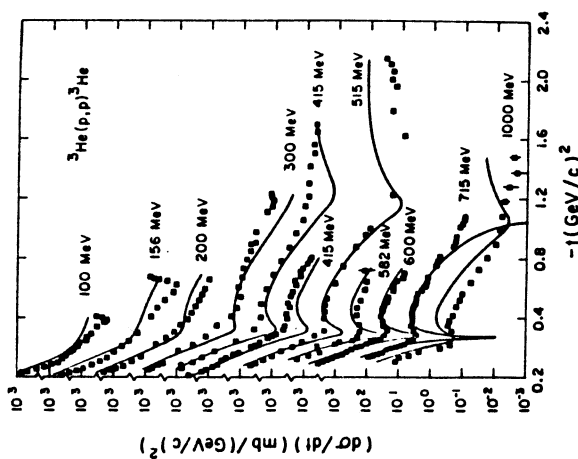


Fig. 3

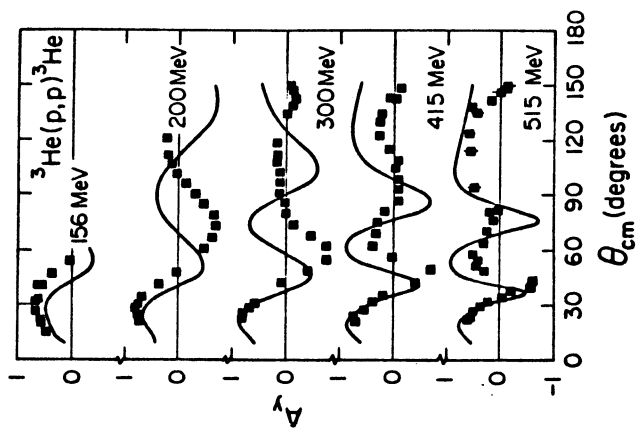


Fig. 5